

The Absence of X-ray Flashes from Nearby Galaxies and the Gamma-Ray Burst Distance Scale

T. T. Hamilton

Department of Astronomy

California Institute of Technology, Pasadena, CA 91125

Electronic Mail: tth@astro.caltech.edu

E. V. Gotthelf¹

Laboratory for High Energy Astrophysics

NASA/Goddard Space Flight Center, Greenbelt, MD 20771

Electronic Mail: gotthelf@gsfc.nasa.gov

and

D. J. Helfand

Department of Astronomy and Columbia Astrophysics Laboratory

Columbia University, 538 West 120th Street, New York, NY 10027

Electronic Mail: djh@carmen.phys.columbia.edu

To appear in the Astrophysical Journal

¹Universities Space Research Association

ABSTRACT

If typical gamma-ray bursts (GRBs) have X-ray counterparts similar to those detected by *Ginga*, then sensitive focusing X-ray telescopes will be able to detect GRBs three orders of magnitude fainter than the detection limit of the Burst and Transient Source Experiment (*BATSE*). If a substantial portion of the burst population detected by *BATSE* originates in a Galactic halo at distances greater than or equal to 150 kpc, existing X-ray telescopes will be able to detect GRBs in external galaxies out to a distance of at least 4.5 Mpc. As reported in Gotthelf, Hamilton, & Helfand (1996) the Imaging Proportional counter (IPC) on board the *Einstein Observatory* detected 42 transient events with pointlike spatial characteristics and timescales of less than 10 seconds. These events are distributed isotropically on the sky; in particular, they are not concentrated in the directions of nearby external galaxies. For halo models of the *BATSE* bursts with radii of 150 kpc or greater, we would expect to see several burst events in observations pointed towards nearby galaxies. We see none. We therefore conclude that if the *Ginga* detections are representative of the population of GRBs sampled by *BATSE*, GRBs cannot originate in a Galactic halo population with limiting radii between 150 kpc and 400 kpc. Inasmuch as halos with limiting radii outside of this range have been excluded by the *BATSE* isotropy measurements, our result indicates that all halo models are excluded. This result is independent of whether the flashes we do detect have an astronomical origin.

Subject headings: gamma rays: bursts - surveys - X-rays: bursts

1. Introduction

Although their existence has been recognized for over two decades, gamma-ray bursts (GRBs) remain enigmatic, their distances and inherent luminosities uncertain by many orders of magnitude. In recent years our understanding has increased enormously as a consequence of the isotropy and apparent luminosity-function measurements carried out by the *BATSE* instrument onboard the *Compton Gamma-Ray Observatory* (CGRO) (Meegan et al. 1992; Hakkila et al. 1994a, 1994b; see Fishman et al. 1989 for a discussion of the *BATSE* experiment). The preponderance of evidence suggests that GRBs originate at one of two possible classes of sites, either in an extended Galactic halo or at cosmological redshifts. Many workers have developed models in which the GRBs arise from a halo population at distances of tens to hundreds of kiloparsecs from the Galactic Center (e.g., Smith & Lamb 1993; Podsiadlowski, Rees, & Ruderman 1995). In this scenario, the observed inhomogeneity in the number-size relation is understood as the result of the finite extent of the halo. The *BATSE* results have effectively excluded models with limiting halo radii of less than 150 kpc (Hakkila et al. 1994a). Other workers have proposed that GRBs originate at cosmological distances. The inhomogeneity is then understood as a result of a combination of evolutionary effects and redshift-induced spectral effects (Paczynski et al. 1986; Paczynski & Rhoads 1993 and references therein).

In this paper we propose and execute a new test of Galactic halo models. We begin with a review of the observed X-ray properties of GRBs and outline our strategy for using existing X-ray imaging data to constrain models of the GRB source distribution (§2). We then define the halo models and construct a catalog of nearby galaxies whose halos were observed by the *Einstein* IPC. Section 4 presents our principal result – the complete absence of bursts from nearby galaxies – and uses this to constrain burst distances. The final section examines the robustness of our conclusions and summarizes our results.

2. X-Rays from GRBs

If our Galaxy is typical, Galactic halo models predict that external galaxies will have sources of GRBs similar to those surrounding the Milky Way, presumably with similar spectral and temporal characteristics. GRBs in these external halos would, of course,

be much fainter than those from the halo of our Galaxy. Because absorption effects will be insignificant over the distances to nearby galaxies, however, measurement of the flux of GRBs from the halo of an external galaxy at a known distance would provide an immediate measure of the intrinsic burst luminosity and, hence, the distance of Galactic GRBs. Similarly, an upper limit on the flux of GRBs in nearby galaxies provides, in the context of halo models, a lower limit on the distance of the *BATSE* detected bursts.

If we assume that the faintest *BATSE* bursts originate at a distance of 150 kpc, the smallest limiting distance consistent with the *BATSE* isotropy tests, it is clear that bursts from galaxies well beyond M31 will be fainter than the *BATSE* limit by orders of magnitude. The only instruments that have any chance of detecting high energy sources at such faint flux levels are focusing X-ray telescopes such as those carried by *Einstein*, *ROSAT* and the *Advanced Satellite for Cosmology and Astrophysics* (*ASCA*). Unfortunately, such telescopes are confined to low energy bands at which *BATSE* spectroscopy is non-existent. We have therefore assumed for the present experiment that typical GRBs have X-ray spectra similar to the spectra of the GRBs observed by *Ginga* (see below). The two largest available databases of X-ray observations are from the *Einstein* and *ROSAT* position sensitive proportional counters. To minimize the uncertainty introduced by the requisite extrapolation from the *Ginga* 1.5 to 10 keV band, we analyze *Einstein* data in preference to the somewhat softer photons recorded in the *ROSAT* database. Nevertheless, the typical X-ray flux associated with GRBs is highly uncertain and remains the greatest source of uncertainty in our experiment. We discuss this in more detail in section 4.

Ginga observed a total of 17 GRBs with a mean flux in the 1.5 – 10 keV band of $\sim 4\%$ that of the gamma-ray flux (Yoshida et al. 1993). Spectral analysis of the brightest of these bursts showed a thermal spectrum with a best fit bremsstrahlung temperature of 1.5 keV (Murakami et al. 1990). While many papers presenting *Ginga* results interpreted them in terms of a blackbody spectral model, this was motivated by the coincidence that the observed *Ginga* burst flux equaled the flux expected from a blackbody with the classical neutron star radius of 10 km at a distance of 1 kpc. The observed *Ginga* spectrum is consistent with that of a 1.5 keV thermal bremsstrahlung continuum. We adopt this model

here, not because we consider it to have any physical significance, but because it is a convenient parameterization of the best data available on GRB X-ray spectra.

The XMON experiment aboard *P78-1* also detected 3-10 keV X-ray counterparts to GRBs, and found flux ratios similar to those detected by *Ginga* (Laros et al. 1984). Both the *Ginga* and XMON results indicate X-ray fluxes somewhat higher than a naive extrapolation of the burst power law spectrum observed between 40 and 70 keV (from the composite of all BATSE bursts – Band et al. 1993). Inasmuch as *Ginga* was only sensitive to the hard portion of this thermal excess, it is possible that the effective temperature is less than the *Ginga* fits with $kT = 1.5$ keV. In that case, the X-ray emission in the *Einstein* IPC band would be greater than we assume here.

No previous experiment has detected absorption of X-rays by material either local to the burst source or lying along the line of sight. However, since our working band is softer, significant absorption could affect *Einstein*-observed bursts. Because most of the galaxies we include in our sample lie in regions of the sky in which Galactic absorption is only $\approx 10^{20}/\text{cm}^{-2}$ (Stark et al. 1992), such line-of-sight absorption is not a major issue. However absorption local to the burst emitter with a column density in the range 10^{21} to 10^{23} cm^{-2} could greatly reduce the source fluence in the IPC band. Such absorbers would have to be physically large (and at least several AU away from the burst) however, in order that the flux from the burst would not fully ionize the absorber, allowing X-rays through.

The composite *Ginga* GRB X-ray spectrum, folded through the *Einstein* spectral response function using the PIMMS software, yields an expected count rate in the *Einstein* IPC of 540 counts per second for a burst with a flux of $2 \times 10^{-7} \text{ erg cm}^{-2}$ in the BATSE band, the limit to which the BATSE team has calculated a reliable number-size relation. Since the background count rate in the IPC is almost always less than one count per thousand seconds per resolution element, an event of a few counts in a ten-second interval stands out dramatically and can easily be detected (Gotthelf, Hamilton, & Helfand 1996, hereafter Paper I). We therefore are sensitive to GRBs out to a distance 30 times greater than the distance of the faintest BATSE bursts.

Both BATSE and our experiment are flux-limited. The longest timescale on which BATSE triggers to

record a burst is 1024 ms, and burst durations range from tens of milliseconds to hundreds of seconds. We are sensitive to X-ray events primarily on a timescale of 1 to 10 seconds and have defined the flux limit of our survey accordingly. If the X-ray bursts are longer than 10 seconds, this is a conservative approach, but if the X-ray counterparts of GRBs frequently had timescales much shorter than 10 s, our flux sensitivity will be proportionately lower than we have estimated. We note that all observed X-ray counterparts of GRBs in fact indicate *longer* timescales for the X-ray emission; indeed, some of the burst we detect have tails extending to 100 s (see figure 1 of Paper I). At higher energies, investigators have also noticed a correlation between softer bursts and longer timescales (Yoshida et al. 1989; Laros et al. 1984; Norris et al. 1986). While these results are not conclusive, we consider that, since *no* observation of a X-ray counterpart to a GRB has detected such an event with a timescale shorter than 10 seconds, we are justified in our sensitivity calculation.

It is possible that events other than GRBs could also produce X-ray flashes in the IPC (Paper I). However, it is not necessary that we understand possible alternative sources of transients in order to test the definite prediction that halo models make regarding extragalactic GRB X-ray counterparts.

3. Halo Models and the Catalog of Galaxies Observed

3.1. Halo Models

The principal interest in the absence of X-ray transients from nearby galaxies is the significance of this non-detection as a test of halo models of GRB sites. The crucial question here is the number of bursts that we would expect to detect if GRBs do originate in the Galaxy's halo. This depends of course on the number of bursts in our Galactic halo and their intrinsic luminosity. We here make the extremely conservative assumption that there are *no* GRBs fainter than those observed by BATSE. We adopt a rate for the Milky Way of 1500 bursts per year. We derive this number from the efficiency calculations of the BATSE team who estimate that BATSE is sensitive to about one quarter of the bursts occurring at the faintest flux levels (Meegan et al. 1994), and apply an additional correction factor of 1.28 to account for our position off-center in the Galactic halo.

The number of bursts expected to be detected by

Einstein is a sensitive function of the limiting halo radius in two ways. If the *BATSE* bursts come from a larger halo, then they are intrinsically more luminous and their X-ray counterparts could thus be detected from more distant galaxies. On the other hand, a more extended halo means that the surface density of bursts in external galaxies will be lower. As a practical matter, given the existence of a limited set of observations in the *Einstein* database, these two effects work against each other. If bursts originate in relatively extended halos, then the number of bursts per unit surface area per unit time will be less for individual galaxies. However, a relatively extended halo implies a relatively high intrinsic burst luminosity. Therefore they can be seen at greater distances and more existing *Einstein* fields would be expected to contain bursts.

We have calculated the expected number of bursts for all halo models consistent with the *BATSE* isotropy result. The adopted lower limit for the limiting burst distance of 150 kpc follows from the upper limit on the GRB quadrupole moment with respect to the plane of the Galaxy, and the upper limit of 400 kpc follows from the upper limit to the dipole with respect to M31 (Hakkila et al. 1994b). We calculate the expected surface density of bursts ρ_s at a distance r from the center of the Galaxy for burst source models in which

$$\begin{aligned} \rho_s &\propto \frac{1}{1+(r/r_c)^\alpha}, & r < r_{lim}, \\ \rho_s &= 0, & r > r_{lim}, \end{aligned}$$

where $\alpha \approx 2$, and the population abruptly cuts off at a radius r_{lim} . This formalism is commonly used in the analysis of *BATSE* data, primarily because it is similar to models of dark matter distributions that are invoked to explain galaxy velocity profiles (Fich & Tremaine 1991; Innanen, Harris, & Webbink 1983). Models in which $\alpha < 2$ can also fit the *BATSE* data and may be physically more reasonable; as shown in Hakkila et al. (1994a), such models require a larger limiting radius. We adopt the model with the conservative assumption that $\alpha = 2$, not because of any belief in its physical significance, but because the use of such a model facilitates interpretation of our results in the context of other GRB studies, especially those interpreting *BATSE* data.

The surface density in such models is not significantly dependent on the value of r_c , the softening parameter in the burst site distribution. For all values of

r_c substantially less than r_{lim} , the expected projected surface density of sources at the center of the halo is $\rho_s = 6.9(D/D_{lim})^2$ per 10^6 seconds deg^{-2} , where D_{lim} is the maximum distance to which a *BATSE* burst at r_{lim} could be detected. For a halo limit of 150 kpc implying $D_{lim} = 4.5$ Mpc, we expect one burst every 145,000 seconds in the *Einstein* field of view. A 150 kpc halo at 4.5 Mpc subtends roughly 10 deg^2 as indeed does any halo of size r_{lim} viewed at the distance corresponding to the limiting sensitivity.

3.2. The Galaxy Catalog

A complete list of nearby galaxies with distances from 1 to 12 Mpc and with $M_v < -16$ was drawn from the *Nearby Galaxies Atlas* (Tully 1989). We have excluded all galaxies that are within 30 arcmin of a brighter galaxy at the same distance in order to ensure that satellite galaxies deep within the halo of a larger galaxy are not counted as independent objects. We have not applied any weighting by mass to the galaxies. In our calculations we have formally assumed that the typical galaxy we observe has a halo identical to that of the Milky Way. The observation times are skewed somewhat towards more luminous galaxies, which were more likely to be chosen as IPC targets for reasons unrelated to our search. This means that assuming all catalog galaxies to be equal contributors to the burst population is a conservative assumption with regard to the distribution of bursts. If we weighted the galaxies, any plausible scheme would place more weight on the systems which were in fact most observed.

This does not, however, resolve the question of the overall normalization of the total galaxy luminosity in our sample. Gott & Turner (1976) estimate that the local density of galaxy optical luminosity is about 2.75 times the optical luminosity density on large scales. Adopting their numbers, we calculate that our assumptions are equivalent to assuming that the burst/galaxy luminosity ratio for our sample is approximately 1.6 times the value for the Galaxy. Specifically, we assume that the total burst-producing material along the line of sight to our sample galaxies has a ratio to those galaxies' luminosity 1.6 times as great as the ratio of burst-producing material within the model radius of the Milky Way to our Galaxy's luminosity. This is roughly comparable to assuming that burst production traces mass and applying standard comparisons of mass to light ratios for galaxies. If a substantial fraction of the intergalactic mass in-

ferred from kinematic studies emits bursts, then the expected bursts will be correspondingly more numerous. Trimble (1987) provides a thorough review of the uncertainties of computing galactic and intergalactic masses in regions with no visible emission. The fact that the mass of material far from the luminous regions of the disk is so uncertain leads us to our simple approach.

We next constructed a database containing all IPC pointings whose centers lay within 5 degrees of any of the 189 galaxies in our catalog, thus including both observations that were deliberately pointed at a nearby galaxy and serendipitous observations in which a galaxy or part of its putative halo is within the field of view. A total of 2.8×10^6 seconds was accumulated, with most of the time spent in scheduled observations of well-known nearby galaxies; one flash was detected. Since *Einstein* detected 18 potentially astronomical flashes in 1.6×10^7 seconds this is not statistically unexpected. This result is not dependent on the arguments used in Paper I to extract the 18 potentially astronomical events from the complete list of 42 candidates; none of the 24 likely counter events fell within the nearby galaxy database. Table 1 lists the galaxy positions, distances and the total time that *Einstein* spent observing a putative 400 kpc halo about each galaxy's position. The observing times for nearby galaxies are large. However, as explained above, the expected surface density of bursts is low for nearby galaxies, and, as a result, most of the contribution to the expected burst total comes from galaxies near the limiting distance for a particular halo model.

Since larger halo models imply higher luminosities for the *BATSE* burst sample, we must examine observations of galaxies at larger distances as the assumed r_{lim} increases. A 200 kpc radius halo would produce bursts visible out to 6 Mpc, while a 400 kpc halo is visible to 12 Mpc and so on. Similarly, the surface density of bursts from the halos of galaxies at distances less than that of the limiting sensitivity is reduced by a factor proportional to the square of the ratio of the distance to the limiting distance.

3.3. Results

Table 2 lists the predicted number of *Einstein*-detected bursts for six model halos with different limiting radii. No X-ray flashes were detected in the halos described by any of these six models.

Column 1 of Table 2 lists the value of r_{lim} in equation 1. Column 2 lists the limiting distance at which bursts can be detected by *Einstein* if the bursts at the *BATSE* flux limit are at a distance r_{lim} . Column 3 lists the total exposure time for all galaxies with $M_v < -16$ whose halos fall within the field of view of an *Einstein* exposure. Column 4 lists the adjusted exposure time. To compute this quantity, the actual exposure time for each halo was reduced by the square of the ratio of the halo's distance to the limiting distance. Note that if galaxies were distributed uniformly in space, column 4 would always equal half of column 3. Columns 5 and 6 give the number of bursts whose detection is expected and the probability that no bursts would be detected if the model applied. Column 7 lists the probability of no bursts being detected if the physical extent of the halo were twice the distance at which *BATSE* is able to detect bursts.

For $r_{lim} = 600$ kpc, bursts would be observable from the Virgo cluster. We would easily see them, since *Einstein* observed in the direction of the cluster for 4,243,000 seconds, often with multiple galaxies in the field of view. Indeed, one burst is seen in the direction of the Virgo cluster (burst # 3 in Table 1 of Paper I). This is consistent with the expected random occurrence rate, and is inconsistent with the 23 bursts from Virgo we would see if typical halos had 600 kpc radii. A halo this large would also produce an anisotropy in the direction of M31 observable with *BATSE* (Hakkila et al. 1994). Our exclusion of such models is therefore an independent confirmation of the M31 results.

We have also considered the possibility that the *BATSE* does not sample the entire extent of the Galactic halo. There is, of course, no reason why the halo could not extend well beyond *BATSE*'s sampling distance. Note that *BATSE*'s non-detection of a dipole towards M31 excludes halos larger than 400 kpc *only* if *BATSE* is able to detect halos that large. That is, *BATSE* obviously can not constrain the location of bursts it cannot see. However, our experiment can test for the existence of halos extended well beyond the *BATSE* limit. Such halos produce many more expected bursts in our galaxy sample and can be readily excluded as seen in Table 2.

We therefore conclude that the GRBs detected by *BATSE* are not associated with X-ray bursts coming from a Galactic halo with a limiting radius greater than 250 kpc and less than 400 kpc, or, equiv-

alently, from bursts with luminosities between $7 \times 10^{38} \text{ ergs s}^{-1}$ and $2 \times 10^{39} \text{ ergs s}^{-1}$ in the 0.16–3.5 keV band. This is the range of halo radii favored by the analysis of Hakkila et al. (1994b). Although our exclusion of halo models with limiting radii as small as 150 kpc is only weakly significant (73%), this result is much stronger if combined with the prior result of Hakkila et al. (1994b). If the GRBs originate in a 150 kpc halo, then three independent probabilities must be considered: 1) this halo radius is at the 90% confidence contour of Hakkila et al.’s (1994b) result; and 2) our result excludes such a halo with 73% confidence; 3) *BATSE* must have been fortuitously designed to see most of the way to the halo’s edge but not beyond. The *a priori* probability of these three independent coincidences is approximately 1%. That is, combining our result with that of Hakkila et al. (1994b) excludes all halo models with $\geq 99\%$ confidence. If we believe that X-ray counterparts are a common feature of GRBs, this would argue strongly for a cosmological GRB origin. The regions of parameter space allowed by Hakkila (1994b)’s results and ours are illustrated in Figure 1. As discussed below this chart uses the conservative and inconsistent assumption that GRBs are standard candles in both the γ -ray and X-ray bands. Deviation from either of these assumptions results in the exclusion of halo models with greater confidence.

4. Robustness of our Conclusion

We consider the uncertainty in the GRB X-ray / γ -ray flux to be easily the weakest link in our argument. Current models for the production of GRBs in a Galactic halo do not predict a sharp low-energy cutoff at the *Einstein* spectral band. Indeed a wide variety of fireball models predict a substantial X-ray excess above what we have used in our calculations (Mészáros & Rees 1993). However, in the absence of a well-established model for the GRB production mechanism, the possibility that GRB spectra suddenly cut-off at the boundary of the *Einstein* and *Ginga* bands cannot be excluded. Unfortunately CGRO does not carry an instrument capable of measuring the spectra of the faint bursts it detects down to X-ray wavelengths. It is likely that in the next few years, however, new experiments will remedy this lack of knowledge and establish definitively the X-ray character of the GRBs.

Closely related to the uncertainty in X-ray / γ -ray

flux ratio is our use of the assumption that GRBs are X-ray standard candles. This is inconsistent with the assumption of Hakkila et al. (1994a) that γ -rays from GRBs are standard candles, because the ratio of X-ray / γ -ray flux is known to vary widely (Yoshida et al. 1989; Laros et al. 1984). Moreover, *BATSE* reports wide variation in the spectrum of the γ -rays it observes (Band et al. 1993). Given this spectral variability it is highly unlikely that any experiment would measure exactly a band in which the GRBs were standard candles.

In the interpretation of both the *BATSE* and IPC results, non-standard candles tend to reduce the parameter space available for halo models. In particular for the IPC result, the assumption of non-standard candles increases the distance at which some bursts could be detected for a given halo model. Since the volume of space from which bursts can be detected with a luminosity L increases as $L^{3/2}$, the total number of detectable bursts increases. In the context of our models this means that bursts four times brighter than average from a, say, 200 kpc radius model would be detected in the galaxy searches performed for the 400 kpc radius model. Inasmuch as the volume searched in the higher radius models includes many more galaxies, non-standard candle models are excluded with higher confidence, just as are the higher radius models. For the 400 kpc model, a factor of two excursion above average in luminosity would result in bursts visible from the Virgo cluster, a result we strongly exclude.

Another implicit assumption of our analysis is that the halos of nearby galaxies resemble that of the Milky Way. The burster halos we are searching for are at galactocentric distances far greater than the visible extent of the galaxy’s light. Consequently, no kinematic evidence exists relevant to the size or frequency of such halos. Even if dark halos were shown to exist about these galaxies, there is no reason to believe that the distribution of GRB source sites would trace the mass distribution. Indeed, halo models that satisfy *BATSE* isotropy constraints show less source concentration toward the center of the Galaxy than halo models derived from rotation curve analysis (Hakkila et al. 1994). Because of the fast time scale of observed GRBs, it is clear they must originate from compact sources. Most models for a Galactic origin of the GRBs postulate an association with neutron stars. Recent observations of neutron star proper motions suggest that the halo may be populated with high

velocity neutron stars that were created during the course of the star formation history of the Galaxy; i.e., they are not primordial (Lyne & Lorimer 1994).

Support for this hypothesis follows from the recent association of supernova remnants with soft gamma repeaters (SGRs) (Murakami et al. 1994). The SGRs appear to be associated with young, high-velocity neutron stars (Rothschild, Kulkarni, & Lingefelter 1994). Perhaps such objects may in time populate an extended halo about any galaxy with an appropriate history of supernovae. If this is the case, it is not completely obvious what types of galaxies would have what types of halos. There may be a complex relationship between mass, galaxy type and halo extent or density. Knowing little, we have followed a simple approach. Because we make the implausible assumption that the *BATSE* detection limit represents an absolute limit on the burst population – i.e., that there are no bursts in our Galaxy below the *BATSE* limit – we consider our estimates to be conservative. However it is obviously possible that our Galaxy is anomalous with respect to its GRB source population.

T. T. H. acknowledges support from NASA grant NAGW-4110 and wishes to thank Fiona Harrison, David Hogg, and Stephen Thorsett for useful discussions. D. J. H. acknowledges support from NASA grant NAS5-32063 and wishes to express his gratitude to his local wine merchant whose case-discount policy has allowed him to avoid bankruptcy in covering his bets that GRBs were Galactic.

REFERENCES

- Band, D., et al. 1993, *ApJ*, 413, 281
- Fich, M. & Tremaine, S., 1991, *ARA&A*, 29, 409
- Fishman, et al. 1989, in *Proc. Gamma-ray Observatory Science Workshop*, ed. W. N. Johnson (Greenbelt: NASA), 2, 39
- Gott, J. R. III & Turner, E. L. 1976, *ApJ*, 209, 1
- Gotthelf, E. V., Hamilton, T. T., & Helfand, D. H. 1996, *ApJ*, in press (Paper I)
- Hakkila, J. et al. 1994a in *Proceedings of the 1993 Huntsville Gamma-Ray Burst Conference*, in press
- Hakkila, J., Meegan, C., Pendleton, G., Fishman, G., Wilson, R., Paciesas, W., Brock, M., & Horack, J. 1994b, *ApJ*, 422, 659
- Innanen, K. A., Harris, W. E., & Webbink, R. F. 1983, *AJ*, 88, 338
- Rothschild, R. E., Kulkarni, S. R., & Lingefelter, R. E. 1994, *Nature*, 368, 432
- Laros, J. G. et al. 1984, *ApJ*, 286, 681
- Lyne, A. G. & Lorimer, D.R., 1994, *Nature*, 369, 127
- Meegan, C. A., Fishman, G. J., Wilson, R. B., Paciesas, W. S., Pendleton, G. N., Horack, J. M., Brock, M. N., & Kouveliotou, C. 1992, *Nature*, 355, 143
- Meegan, C. A., et al. 1994, Status report available from gronews@grossc.gsfc.nasa.gov
- Mezaños, P. & Rees, M. 1993, *ApJ*, 418, L59
- Murakami, T., et al. 1991, *Nature*, 350, 592
- Murakami, T., et al. 1994, *Nature*, 368, 127
- Norris, J. P., Share, G. H., Messina, D. C., Dennis, B. R., desai, U. D., Cline, T. L., Matz, S. M., & Chupp, E. L., 1986, *ApJ*, 301, 213
- Paczynski, B. 1986, *ApJ*, 308, L43
- Paczynski, B. & Rhoads, J. 1993, *ApJ*, 418, L5
- Podsiadlowski, P., Rees, M., & Ruderman, M. A., 1995, *MNRAS*, 273, 755
- Smith, I. A. & Lamb, D. Q. 1993, *ApJ*, 410, L23
- Stark, A. A., et al. 1992 *ApJS*, 79, 77
- Tully, B. 1988, *Nearby Galaxies Catalog* (Cambridge: Cambridge Univ. Press)
- Trimble, V. 1987 *ARA&A*, 25, 425
- Yoshida, A., et al. 1989, *PASJ*, 41, 509

TABLE 1
LIST OF GALAXIES

Right Ascension (1950)	Declination (1950)	Distance (Mpc)	Time (s)	Right Ascension (1950)	Declination (1950)	Distance (Mpc)	Time (s)
Galaxies at 4–12 Mpc				05 09 36	62 31	4.5	14821
00 43 18	- 15 52	11.6	0	05 10 06	- 33 02	10.2	0
00 49 18	47 17	11.8	0	05 13 42	53 30	11.4	0
01 27 12	- 01 30	10.6	12888	05 45 12	- 34 15	10.2	9656
01 34 00	15 32	9.7	6867	05 33 06	03 24	10.3	0
01 39 42	13 43	10.8	0	06 08 24	- 34 06	7.9	1921
01 40 18	13 23	11.8	0	03 27 00	39 31	8.6	0
01 44 42	27 05	6.4	8339	07 06 36	44 32	8.2	2610
01 45 00	27 11	7.5	8339	07 32 06	65 43	4.2	82623
01 46 42	32 20	4.6	72619	07 35 00	- 47 31	10.9	0
01 58 24	28 35	4.7	16197	07 58 12	50 54	10.1	0
02 19 18	42 07	9.6	10364	08 09 42	46 09	9.0	8390
02 21 54	35 49	9.8	6335	08 10 24	45 54	10.6	0
02 24 18	33 22	9.4	10474	08 11 00	49 13	10.6	8390
02 27 48	36 55	10.3	0	08 14 06	70 52	4.5	57834
02 29 18	35 17	10.1	6335	08 15 42	50 10	10.0	8390
02 30 18	33 17	10.1	6335	08 49 36	33 38	5.7	13479
02 30 36	40 19	10.2	2748	08 55 48	39 24	8.7	4249
02 33 24	25 13	10.7	1432	09 04 24	33 28	7.8	1319
02 36 06	40 40	10.7	2748	09 10 06	- 23 58	7.1	6102
02 37 18	38 51	10.5	2748	09 15 42	- 22 09	10.8	6102
02 37 42	19 05	11.2	1972	09 18 36	51 12	12.0	0
02 40 12	37 08	9.1	1629	09 29 24	21 44	6.3	11298
02 44 48	37 20	10.0	1629	09 51 42	69 55	5.2	37258
02 55 24	- 54 46	5.4	5900	10 00 54	41 00	9.4	0
02 56 48	25 02	6.4	9961	10 02 42	- 07 29	6.7	4111
03 08 36	- 53 32	10.7	5900	10 15 12	41 40	8.7	614
03 15 30	- 41 19	8.6	2809	10 16 42	45 49	10.8	0
03 24 18	- 52 57	11.5	10890	10 22 24	17 25	8.1	8496
03 30 12	- 52 05	11.6	6436	10 36 24	41 56	11.5	0
03 31 54	- 31 22	11.6	562	10 40 48	25 11	6.1	0
03 37 06	- 44 15	11.2	2016	10 41 18	11 58	8.1	29026
03 37 18	- 18 51	5.0	26936	10 43 42	02 05	10.7	2576
03 37 30	- 31 30	11.8	1646	10 44 12	12 05	8.1	29026
03 40 30	- 47 23	11.6	0	10 45 06	14 15	8.1	20724
03 55 54	- 46 21	11.3	2016	10 45 12	12 51	8.1	20724
04 01 54	- 02 19	10.6	915	10 45 36	12 54	8.1	26872
04 01 54	- 43 33	10.3	2052	10 48 18	13 41	8.1	28961
04 02 18	- 43 29	9.5	2052	10 48 00	76 07	10.9	3767
04 06 54	- 48 01	11.0	0	10 49 42	36 54	7.8	9728
04 38 54	- 02 56	8.9	5975	10 57 42	14 10	6.4	42074
04 53 06	- 53 27	6.0	14185	10 57 48	29 15	7.4	14465
04 57 54	- 26 06	7.8	1448	11 01 00	29 09	7.9	16049
05 02 06	- 61 12	10.6	0	11 03 12	00 14	7.2	0
05 04 30	- 32 01	7.4	0	11 17 36	13 17	6.6	20902
05 06 00	- 37 35	10.8	0	11 17 42	13 53	7.7	20902
05 08 48	- 31 40	10.8	0	11 33 00	54 47	4.3	39312
				11 54 06	48 36	8.3	4617

TABLE 1 (CONTINUED)

Right Ascension (1950)	Declination (1950)	Distance (Mpc)	Time (s)		Right Ascension (1950)	Declination (1950)	Distance (Mpc)	Time (s)
11 56 18	30 41	8.0	9593		13 16 18	- 20 47	6.7	12865
12 01 30	32 11	9.7	3595		13 22 24	- 42 45	4.9	72177
12 03 30	47 45	8.8	533		13 27 42	58 40	4.8	39344
12 06 42	30 12	9.7	12809		13 27 48	47 27	7.7	0
12 07 30	46 44	4.1	23065		13 34 12	- 29 37	4.7	53825
12 08 00	30 41	9.7	8471		14 01 30	54 36	5.4	62760
12 09 48	29 28	9.7	23093		14 03 18	53 54	6.0	61442
12 12 36	33 29	9.7	8669		14 09 18	- 65 06	4.2	62192
12 12 42	20 56	7.9	9176		14 18 12	56 57	7.0	42017
12 14 54	45 54	7.5	12264		15 27 12	64 55	11.2	12942
12 15 06	29 53	9.7	17095		17 49 54	70 10	6.1	203860
12 15 24	47 41	7.3	3120		18 23 30	- 67 01	8.9	2575
12 15 36	28 27	9.7	17095		18 44 06	- 65 14	10.9	17959
12 16 30	47 35	6.8	3120		20 33 48	59 59	5.5	27662
12 17 24	29 53	9.7	17095		20 47 24	- 69 24	6.7	85610
12 17 36	29 34	9.7	17095		21 25 36.01	- 52 59	10.6	0
12 17 48	29 35	9.7	17095		21 33 00	- 54 47	10.4	0
12 18 12	46 35	8.0	4788		22 01 30	43 30	10.5	49241
12 19 54	29 29	9.7	17095		22 18 18	- 46 19	11.1	0
12 20 06	30 10	9.7	22317		23 19 42	40 34	8.6	1850
12 21 36	31 48	9.7	15083		23 22 18	41 04	9.3	1850
12 22 06	70 37	11.1	17904		23 27 36.01	40 43	9.2	1850
12 23 18	27 50	9.7	12295		23 31 48	- 36 22	8.4	4142
12 24 00	31 30	9.7	10022		23 33 36.01	- 38 12	8.2	2630
12 25 48	28 54	9.7	12295		Galaxies at 1–4 Mpc			
12 26 12	23 06	6.2	17168		00 44 36	- 21 01	2.1	33505
12 26 24	45 09	8.1	4255		00 45 06	- 25 34	3.0	29926
12 28 12	41 58	9.3	6523		00 52 30	- 37 57	1.2	116295
12 28 18	41 55	7.8	8693		01 06 42	35 27	2.4	111305
12 28 54	26 03	9.7	4200		01 32 54	- 41 40	3.9	46641
12 30 00	42 59	7.5	6523		03 17 42	- 66 41	3.7	7988
12 30 12	00 23	9.8	10561		03 42 00	67 56	3.9	8081
12 30 24	37 54	6.2	31129		04 26 00	64 45	1.6	27389
12 31 18	30 34	9.7	5222		04 27 06	71 48	3.0	12895
12 31 42	35 48	9.8	2311		07 23 36	69 18	2.9	100820
12 33 30	28 14	9.7	0		09 43 12	68 8	2.1	116847
12 33 48	26 15	9.7	2692		09 51 30	69 18	1.4	238546
12 36 42	00 16	9.6	4298		09 59 24	68 59	2.1	134772
12 39 12	41 25	7.3	4855		10 00 48	- 25 55	1.8	12750
12 39 48	32 49	6.9	15415		10 24 48	68 40	2.7	80551
12 41 36	32 26	7.2	10193		12 13 06	36 36	3.5	94632
12 46 6	51 26	8.0	1227		12 14 18	69 45	2.2	113804
12 48 36	41 23	4.3	13566		12 15 00	38 05	3.1	107833
12 54 18	21 57	4.1	18018		12 23 24	33 49	3.6	128582
13 00 42	- 17 08	7.1	20254		12 25 48	44 22	3.0	85825
13 01 36	- 05 17	6.4	40986		13 19 06	- 36 22	3.5	63770
13 02 30	- 49 12	5.2	24633	10	13 37 06	- 31 24	3.2	55790
13 10 00	44 18	6.0	6201		17 42 12	- 64 37	3.0	25746
13 13 30	42 17	7.2	6201		23 55 18	- 32 51	2.8	37713

TABLE 2
HALO MODELS

r_{lim} (kpc)	D_{lim} (Mpc)	Total Time (ksec)	Adjusted Time (ksec)	Expected Events	Significance	Probability of Doubled Radius
150	4.5	391	208	1.4	.239	0.027
200	6.0	638	292	2.0	.135	0.004
250	7.5	1020	470	3.2	.041	< 0.0001
300	9.0	1290	606	4.2	.015	< 0.0001
350	10.5	1590	829	5.7	.003	< 0.0001
400	12.0	1890	915	6.3	.002	< 0.0001

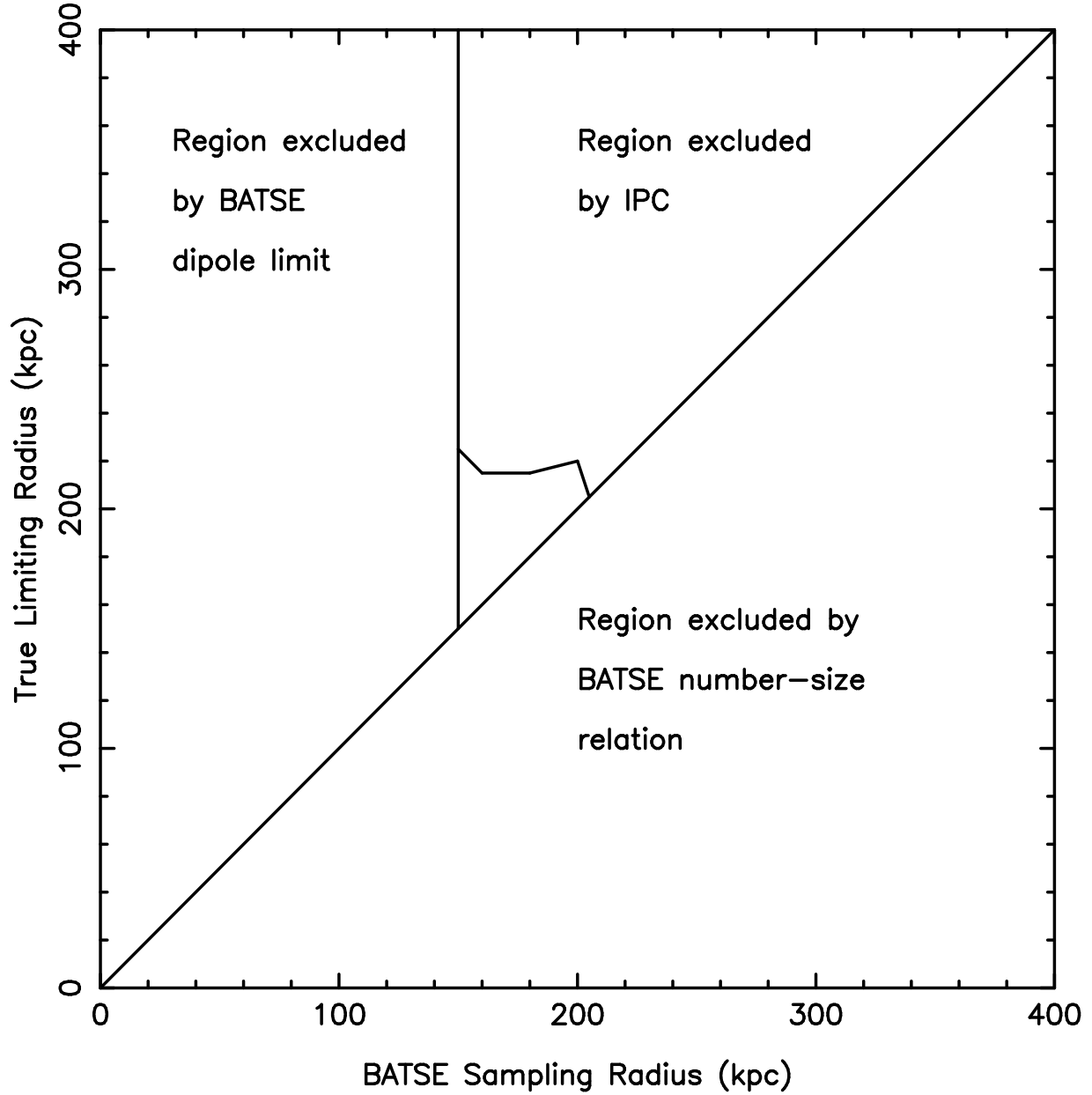


Fig. 1.— The region of parameter space of possible halo models excluded with $> 90\%$ confidence by various experiment is plotted. The abscissa is the distance of the faintest bursts detected by *BATSE* and the ordinate is the distance of the faintest bursts which exist. We have assumed standard candles and a continuation of the $\text{Log } N - \text{Log } S$ below the *BATSE* limit with the same slope. We allow the inner radius of the distribution to assume any value. For *BATSE* models in the area not excluded by any one experiment, that radius is about 20 kpc. The irregular shape of the IPC contour is a result of the finite number of nearby galaxies.